IEEE Access
Multidisciplinary ⋮ Rapid Review ⋮ Open Access Journal

Received 8 October 2024, accepted 10 November 2024, date of publication 15 November 2024, date of current version 27 November 2024.

Digital Object Identifier 10.1109/ACCESS.2024.3499352

RESEARCH ARTICLE

Optimizing a Hybrid Controller for Automotive Active Suspension System by Using Genetic Algorithms With Two High Level Parameters

VU VAN TAN[1], DO TRONG TU[2], NGUYEN VAN VINH[1], PHAM TAT THANG[1], ANDRAS MIHALY[3], AND PETER GASPAR[3]

[1]Department of Automotive Mechanical Engineering, Faculty of Mechanical Engineering, University of Transport and Communications, Hanoi 100000, Vietnam
[2]Faculty of Mechanical-Automotive and Civil Engineering, Electric Power University, Bac Tu Liem, Hanoi 100000, Vietnam
[3]Systems and Control Laboratory, Institute for Computer Science and Control, Hungarian Research Network, 1111 Budapest, Hungary

Corresponding authors: Vu Van Tan (vvtan@utc.edu.vn) and Andras Mihaly (mihaly.andras@sztaki.mta.hu)

This work was supported by the National Research, Development, and Innovation Office through the Project "Cooperative emergency trajectory design for connected autonomous vehicles" under Grant NKFIH: 2019-2.1.12-TÉT_VN.

ABSTRACT This article presents the in-depth research results concerning the actively controlled suspension system following the Hybrid Active Suspension System (HASS) in vehicles. Initially, detailed introductions are provided for the controller and actuator of this suspension system model. Afterward, the HASS model is proposed for application to the Active Suspension System with integrating Skyhook and Groundhook control methods, wherein a coefficient $\alpha = 0.3,\ 0.6,\ 0.9$ is utilized to adjust the correlation between these two models. Through the amplitude transfer function, the transition in enhancing ride comfort and road holding criteria in the HASS is demonstrated. Subsequently, the coefficients of the HASS are optimized through the Genetic Algorithm optimization with the parameter $\beta = 0.1,\ 0.5,\ 0.9$, aiming to enhance ride comfort and road holding corresponding to each value of α. The simulation and evaluation results utilizing the HASS in both frequency and time domains demonstrate significant improvements in ride comfort and road holding criteria compared to passive suspension systems. Specifically, the ride comfort has improved from 60% to 80%, while the road holding has improved from 10% to 15%. These findings facilitate the development of applications for the controlled suspension system, allowing adaptation to diverse real-world conditions at varying levels.

INDEX TERMS Vehicle dynamics and control, active suspension system, hybrid active suspension system, Skyhook model, Groundhook model, genetic algorithm optimization, suspension system.

I. INTRODUCTION

The suspension system, which is one of the primary systems in vehicles, is designed to connect and support the vehicle body on the wheels and isolate vibrations induced from the road surface. This system consists of two main elements: the spring element commonly constructed with coil springs or leaf springs or air springs, and the damping element usually hydraulic shock absorbers with one or two layers of shells [1]. These components are typically designed based on input conditions such as the load impacting the suspension system and the desired oscillation frequency. Therefore, the vibration quality of the vehicle is satisfied under certain operational constraints [2]. To overcome this limitation, controlled suspension systems are studied and developed in two main forms: Active Suspension System (ASS) and semi- Active Suspension System (sASS) [1], [2]. The sASS is typically comprised of a spring element and a damping element that can be adjusted for the damping coefficient. This system has the advantage of being cost-effective and effective in improving vibration quality up to a certain threshold. However, the drawbacks of this system are generating relatively low damping force and not covering all operational conditions of the vehicle [3], [4].

The associate editor coordinating the review of this manuscript and approving it for publication was Christian Pilato.

The ASS has been developed and incorporated into commercial vehicles by automotive manufacturers and researchers. This system utilizes an actuator that enables control of various modes to enhance the vibration quality of the vehicle [5], [6]. Although there have been some studies on the configuration, models, and control approaches for this system, more detailed research is needed to refine the system for heavy-duty vehicles such as buses and trucks. The ASS in vehicles operates based on controlling the actuator, which is connected between the unsprung mass and the sprung mass, to minimize road-induced dynamic forces and increase ride comfort for the driver and passengers. Below is a summary of the main research directions regarding this system:

A. SUSPENSION SYSTEM MODEL IN VEHICLES

Currently, theoretical, and experimental research is utilizing three common suspension models in vehicles: quarter-vehicle, half-vehicle, and full-vehicle [1], [2]. The general quarter- vehicle suspension system model is composed of the following components: sprung mass, unsprung mass, damper, spring, and the tire, which is considered as a spring, contacts with the ground without experiencing the effects of friction [7], [8]. For the ASS system, the actuator is arranged in parallel with the damper element and the spring element to generate the control force. Unlike the quarter model, which only is affected by road irregularities at one wheel, the half-vehicle model considers the unsprung mass element with two wheels (one front and one rear wheel for a pitch model, or one left and one right wheel for a roll model). The main advantage of this type of model is its ability to consider the pitch or roll motion of the vehicle body; the damping and spring characteristics can be modeled in different ways according to the type of suspension systems (dependent or independent), which is also suitable for real-world vehicles [9]. The full-vehicle model includes the vehicle sprung mass connected by the suspension system with four wheels (unsprung mass). Each ASS is modeled as an adjustable transmission system, while the wheel is modeled as a linear spring. The vehicle sprung mass can oscillate vertically, pitch, and roll axles, while the wheels only move in a vertical direction relative to the vehicle sprung mass [1], [4]. Although the half-car and full-car models have the advantage of accurately describing the dynamic characteristics of vehicles, their complexity and numerous constraints make control design challenging. Depending on the specific research objectives, compatible model forms will be employed. In this regard, for research on new control strategies, authors often use the quarter model for model simplification while still ensuring the characteristics of the vehicle oscillation.

B. THE CONTROL METHOD FOR ACTIVE SUSPENSION SYSTEM

To control the actuator of ASS, the designed controller has many types such as control based on the Skyhook or Groundhook prototypical [10], [11], PID control [12], [13], [14], optimal control LQR/LQG [15], [16], [17], [18], [19], robust control with LTI or LPV models, nonlinear control [20], [21], [22], neural network [23], [24], [25]...Control methods can be divided into three groups:

Group 1: model-based control group such as Skyhook, Groundhook. In this group, there must always exist two types of models: the control object model and the ideal model. The control strategies must be built so that the total force or moment effect on the control object model must be the same as in the ideal model.

Group 2: control group based on information from dynamic models of the system such as LQR, LQG, H_∞. In this group, the control strategies are designed based on the control objective and it depends entirely on the parameters of the control object model.

Group 3: control group which is independent of model parameters but dependent on control objectives such as PID, Fuzzy logic [26], [27], [28].

Control based on models like Skyhook or Groundhook has the advantage of predefining control models based on the designer's experience, thereby limiting constraints beyond the control objectives. However, this control method has the disadvantage of limited flexibility and difficulty in covering complex motion vehicle behaviors [1], [3].

Control based on dynamic models such as LQR, LQG, and H_∞ is a concern to authors because it has the advantage of creating accurate compatibility with the research objects, generating diverse control objectives through various approaches [20]. However, its drawbacks arise from its characteristics in the real-time system state, because it is very difficult to precisely determine the parameters of the real car model. To overcome these troubles, the H_∞ control method allows for the utilization of the uncertain feature of parameters [22], [29], [30].

Control methods that are independent of system parameters such as PID and Fuzzy have many advantages for highly complex objects like vehicle oscillations. These methods require the determination of control objectives and experience with system characteristics. For PID control, setting up the controller is relatively simple and easy to implement, but accurately tuning the K_P, K_I, K_D coefficients to minimize control objectives and balance with the physical characteristics of the actuation mechanism still encounters many difficulties [12]. Fuzzy control has the advantage of considering the unclear characteristics of the system according to experience, but it also raises significant issues regarding accuracy and requires a high level of design [31].

C. THE OPTIMIZATION METHOD IN SUSPENSION SYSTEM

To enhance the oscillation quality of suspension systems, in general, and ASS, in particular, various optimization methods are studied and applied, such as swarm optimization [32], robust optimization [33], and Genetic Algorithm (GA) optimization [34]. These approaches are considered for the following issues: optimizing the stiffness of the spring

element and the damping coefficient of the shock absorber (for the conventional suspension system); actuator saturation, time delay, and state constraint (for the controlled suspension system) [35]. Some studies utilize these techniques to determine the parameters of PID, and LQR controllers to enhance their effectiveness. However, most of these optimization problems only focus on determining optimal solutions for specific oscillation approaches without solving the overall problem considering different objectives such as ride comfort and road holding [13], [32], [36], [37].

This research concentrates on establishing a novel approach to controlling ASS in heay-duty vehicles by employing the HASS model and optimizing model parameters through the GA optimization method. By considering the research scope in the two main vibration criteria of the ride comfort and the road holding, the main contributions are listed as follows:

- The HASS is established through the combination of two typical models: Skyhook aiming to enhance ride comfort, and Groundhook aiming to improve road holding. The roles of these two models are interchanged through a single-coefficient α for the quarter-vehicle model.

- The characteristics of the HASS are examined through the amplitude transfer function of the vehicle sprung mass and the dynamic tyre force impacting the road with various values of the coefficient $\alpha = [0 \div 1]$.

- The GA method is applied to optimize the parameters of the Hybrid controller while considering the variation of the coefficient β related to ride comfort and road holding. The optimized results and evaluations confirm the superiority of this entirely novel approach to research by combining GA and HASS in vehicles.

The structure of the paper is organized as follows: Section II describes the ASS in heavy-duty vehicles; Section III proposes a HASS for the ASS and its characteristics; Section IV presents the evaluation results surveying the impact of the HASS parameters on the vehicle; Section V describes the application of GA to optimize the HASS; The validation results between the proposed HASS integrated GA for the trade-off criteria on vehicle is demonstrated in Section VI.

II. ACTIVE SUSPENSION SYSTEM IN VEHICLES

The passive suspension system, in modern vehicles, is primarily composed of two main components: the spring element and the damping element. These components are designed according to each type of vehicle and based on their respective technical specifications. Within the usual operating ranges, the stiffness of the spring element and the damping coefficient of the damping element are often considered as constants. However, the damping coefficient can cause a contradiction between the road holding and the ride comfort of the vehicle. A low damping coefficient increases ride comfort but decreases road holding, whereas a high damping coefficient increases road holding but decreases ride comfort as described in Figure 1 [1], [6]. When the damping coefficient is low, it means that the fluid can easily pass through the throttle holes inside the damper. This will create less force to dampen the oscillations, making the sprung mass smoother, but this has the disadvantage of the unsprung mass tending to reduce the connection with the road surface.

The road holding of the vehicle is primarily limited by the vertical displacement of the wheels, the rotational displacement of the vehicle body, and the pitch and/or roll angles of the vehicle body during braking or cornering. In contrast, the ride comfort of the vehicle can be assessed through the vertical displacement, pitch angle, roll angle and their accelerations of the vehicle body.

The primary source of vehicle oscillation is caused by the road profile. Currently, passive suspension systems are considered optimal only for certain types of roads. Therefore, to meet the ride comfort and road holding criteria on all types of roads, the characteristics of the suspension system need to change during vehicle state to be appropriate for the road characteristics. ASS can adapt to various vehicle motion conditions, as illustrated in Figure 2a). The fundamental parameters of the ASS include: Z_s- Displacement of sprung mass; Z_u- Displacement of unsprung mass; C_s - Stiffness of the spring element; K_s - Damping coefficient; C_t- Tyre stiffness coefficient; K_t - Tyre damping coefficient; q- Road profile. The ASS consists of an electronic servo-valve hydraulic actuator that can generate the force F_{act}, a controller that enables automated and precise management of complex systems, and sensors that detect and respond to various types of physical stimuli. This suspension system is effective but requires a large energy supply. The dynamics equation of the vehicle model using the ASS is defined as follows:

$$\begin{cases} m_u\ddot{Z}_u - K_s\left(\dot{Z}_s - \dot{Z}_u\right) - C_s\left(Z_s - Z_u\right) + K_t \\ \left(\dot{Z}_u - \dot{q}\right) + C_t\left(Z_u - q\right) = F_{act} \\ m_s\ddot{Z}_s + K_s\left(\dot{Z}_s - \dot{Z}_u\right) + C_s\left(Z_s - Z_u\right) = -F_{act} \end{cases} \quad (1)$$

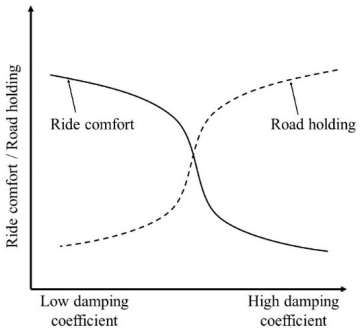

FIGURE 1. The influence of the damping coefficient on the trade-off on the vehicle: ride comfort and road holding [1], [6].

Figure 2b) illustrates the structure of the actuator consisting of a hydraulic cylinder combined with an electronic servo-valve. This valve is controlled by an electric current u for its displacement X_v. The high-pressure oil P_s is always

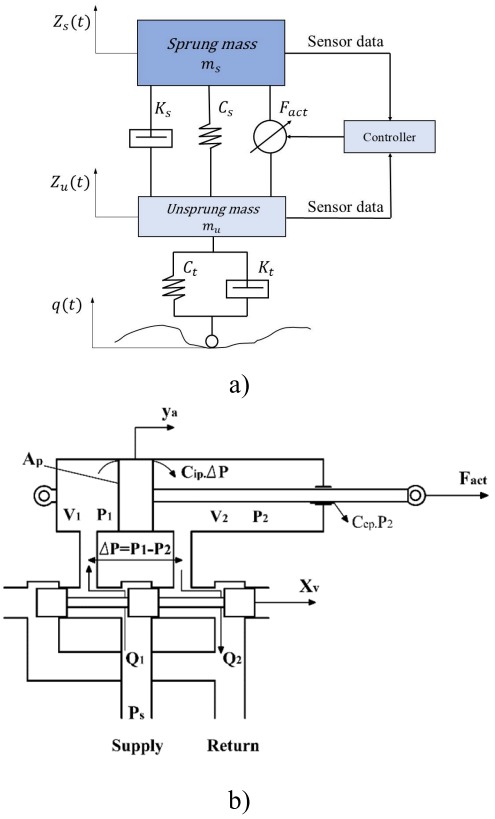

FIGURE 2. The active suspension system model on vehicles: a) Layout diagram, b) Hydraulic-electric actuator.

stored outside the electromagnetic valve. Through the displacement of the servo-valve, the high-pressure oil flow is divided into two branches leading to the two chambers of the hydraulic cylinder. The difference pressure $\Delta P = P_1 - P_2$ between the two chambers generates the force of the hydraulic cylinder F_{act}. Consequently, this actuator has an input signal of amperage u and an output signal of force F_{act}, the relationship of them is expressed in equation (2).

$$\begin{cases} F_{act} = A_P \Delta P \\ \dfrac{V_t}{4\beta_e}\dfrac{d\Delta P}{dt} + \left(K_P + C_{tp}\right)\Delta P - K_x X_v + A_P \dfrac{dy_a}{dt} = 0 \\ \dfrac{dX_v}{dt} + \dfrac{1}{\tau}X_v - \dfrac{K_v}{\tau}u = 0 \end{cases} \tag{2}$$

III. HYBRID ACTIVE SUSPENSION SYSTEM CONTROL FOR VEHICLES

A. HYBRID CONTROL MODEL

The HASS in vehicles is described in Figure 3, posits that the sprung mass will be connected to an imaginary fixed point through damping with a coefficient K_{sky} (according to the Skyhook model), and the unsprung mass will be connected to another imaginary fixed point through damping with a coefficient K_{grd} (according to the Groundhook model). From Figure 2a), it can be observed that the ASS will continuously adjust the force F_{act} of the actuator over time so that its impact force on both the sprung and unsprung masses is equivalent to the sum of the two imaginary damper forces as shown in Figure 3. The parameters of the 2 models (Figure 2a, Figure 3) are presented in Table 1 [38].

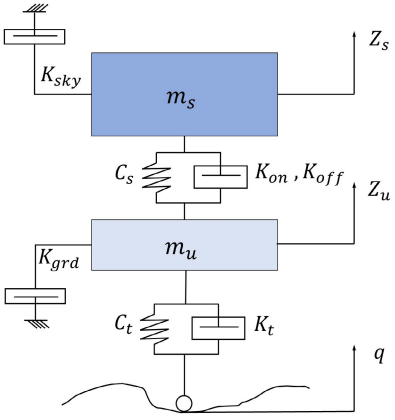

FIGURE 3. Hybrid control model.

The dynamic equation of the 1/4 vehicle model utilizing HASS is determined in equation (3) and expressed in matrix form as in equation (4).

$$\begin{cases} m_s\ddot{Z}_s + K_{sky}\dot{Z}_s + K_{off}(\dot{Z}_s - \dot{Z}_u) + C_s(Z_s - Z_u) = 0 \\ m_u\ddot{Z}_u - K_{off}(\dot{Z}_s - \dot{Z}_u) - C_s(Z_s - Z_u) + K_t(\dot{Z}_u - \dot{q}) \\ +C_t(Z_u - q) + K_{grd}\dot{Z}_u = 0 \end{cases} \tag{3}$$

$$[M]\ddot{Z} + [K]\dot{Z} + [C]Z = [A]\dot{q} + [B]q \tag{4}$$

where: q - road profile; Z - displacement vector of the system; $[M]$ - mass matrix; $[K]$ - damping coefficient matrix; $[C]$ - stiffness matrix. These matrices are defined as follows:

$$[M] = \begin{bmatrix} m_s & 0 \\ 0 & m_u \end{bmatrix};$$
$$[K] = \begin{bmatrix} K_{off} + K_{sky} & -K_{off} \\ -K_{off} & K_{off} + K_t + K_{Grd} \end{bmatrix};$$
$$[C] = \begin{bmatrix} C_s & -C_s \\ -C_s & C_s + C_t \end{bmatrix}; [A] = \begin{bmatrix} 0 \\ K_t \end{bmatrix}; [B] = \begin{bmatrix} 0 \\ C_t \end{bmatrix};$$
$$Z = \begin{bmatrix} Z_s \\ Z_u \end{bmatrix}.$$

B. MAGNITUDE TRANSFER FUNCTION OF SIGNAL IN FREQUENCY DOMAIN ACCORDING TO THE HYBRID CONTROL MODEL

The road profile function is a time-harmonic function defined by equation (5), where: q_0 - amplitude of the road profile; ω - frequency of excitation; j- imaginary unit; t- time of excitation.

$$q = q_0 e^{j\omega t} \tag{5}$$

TABLE 1. Table of parameters for the 1/4 model with HASS [38].

Symbol	Parameter	Value	Unit
m_s	Sprung mass	8900	Kg
C_s	Spring stiffness	2000000	N/m
K_{on}	Maximum damping coefficient	350000	Ns/m
K_{off}	Minimum damping coefficient	0	Ns/m
m_u	Unsprung mass	1100	kg
C_t	Tyre stiffness	3500000	N/m
K_t	Tyre damping coefficient	4000	Ns/m
α	Correlation coefficients	0÷1	-

The displacement vector of the system also takes the form of a harmonic function as in the following equation.

$$Z = Z_0 e^{j\omega t} \tag{6}$$

where $Z_0 = [Z_{so} Z_{uo}]^T$ is the displacement amplitude vector.

From equations (4), (5), (6), we have the dynamic equation of the model as follows:

$$\begin{aligned} &\left(-[M]\omega^2 + j[K]\omega + [C]\right) Z_0 \\ &= (j[A]\omega + [B])\, q_0 \end{aligned} \tag{7}$$

$$\begin{aligned} \frac{Z_0}{q_0} &= \left(-[M]\omega^2 + j[K]\omega + [C]\right)^{-1} (j[A]\omega + [B]) \\ &= H_z(\omega) \end{aligned} \tag{8}$$

$H_z(\omega) = \left(-[M]\omega^2 + j[K]\omega + [C]\right)^{-1} (j[A]\omega + [B])$ is referred to as the displacement transfer function matrix of the system. The acceleration transfer function matrix is determined as follows:

$$\begin{aligned} &H_{\ddot{Z}}(\omega) \\ &= \frac{\ddot{Z}_0}{q_0} = \frac{-Z_0\omega^2}{q_0} \\ &= -\omega^2 \left(-[M]\omega^2 + j[K]\omega + [C]\right)^{-1} (j[A]\omega + [B]) \end{aligned} \tag{9}$$

The dynamic tyre force acting on the road surface is determined by [6]:

$$F_{dt} = \ddot{Z}_s m_s + \ddot{Z}_u m_u \tag{10}$$

From equation (10), dividing both sides by the road profile (q), we obtain the transfer function of the dynamic tyre force in equation (11):

$$\begin{aligned} H_{F_{dt}} &= H_{\ddot{Z}_s} m_s + H_{\ddot{Z}_u} m_u \\ &= \begin{bmatrix} m_s & m_u \end{bmatrix} \begin{bmatrix} H_{\ddot{Z}_s} \\ H_{\ddot{Z}_u} \end{bmatrix} = \begin{bmatrix} m_s & m_u \end{bmatrix} H_{\ddot{Z}} \end{aligned} \tag{11}$$

C. ACTIVE SUSPENSION SYSTEM CONTROL ACCORDING TO THE HYBRID ACTIVE SUSPENSION SYSTEM

When increasing the damping Skyhook and Groundhook coefficients in the HASS model, the wheel displacement amplitude and the sprung mass acceleration decrease. Survey results indicate that the parameter $\alpha = 0.6 \div 0.7$ is optimal for both ride comfort and road holding. The ASS controlled by the model in Figure 2a) with a damper-controlling equation according to the HASS is proposed as in equation (12):

$$\begin{cases} \alpha \dot{Z}_s \left(\dot{Z}_s - \dot{Z}_u\right) - (1-\alpha)\, \dot{Z}_u \left(\dot{Z}_s - \dot{Z}_u\right) \geq 0 \\ \Rightarrow F_{SA} = G\left[\alpha \dot{Z}_s K_{sky} + (1-\alpha)\, \dot{Z}_u K_{grd}\right] \\ \alpha \dot{Z}_s \left(\dot{Z}_s - \dot{Z}_u\right) - (1-\alpha)\, \dot{Z}_u \left(\dot{Z}_s - \dot{Z}_u\right) < 0 \\ \Rightarrow F_{SA} = 0 \end{cases} \tag{12}$$

where: α is the correlation parameter of the Skyhook model through the damping coefficient K_{sky}, chosen appropriately between controlling the unsprung mass and the sprung mass. When $\alpha = 1$ the HASS becomes the pure Skyhook model, when $\alpha = 0$ the model becomes the pure Groundhook model. The coefficients K_{sky} and K_{grd} are determined as follows:

$$K_{sky} = \alpha \left(K_{on} - K_{off}\right) \text{ and } K_{grd} = (1-\alpha) \left(K_{on} - K_{off}\right)$$

The F_{SA} force in equation (12) is the control force according to the hybrid model, this force is identified with the F_{act} force of actuator in equation (2) to be included in the vehicle model in Figure 2a.

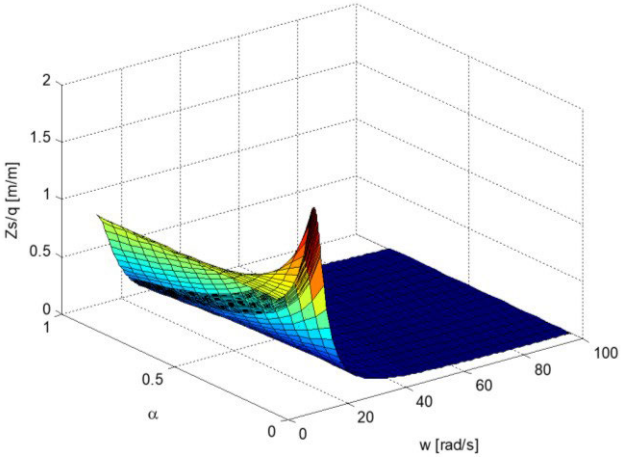

FIGURE 4. Frequency-response characteristics of sprung mass displacement.

Figures 4, 5, and 6 illustrate the transfer function of displacement, acceleration, and dynamic tyre force when the parameter changes from 0 to 1, demonstrating the trade-off on 4 heavy vehicle model, namely road holding and ride comfort. It can be observed that as the varying parameter α, the characteristics of the vehicle's transfer function vary with different excitation frequencies.

IV. EVALUATING THE INFLUENCE OF K_{sky} AND K_{grd} ON THE HYBRID ACTIVE SUSPENSION SYSTEM

In this section, the authors propose a HASS combining the Skyhook and Groundhook models for the ASS to enhance the suspension system performance under various operating conditions. The Skyhook mode focuses on improving ride

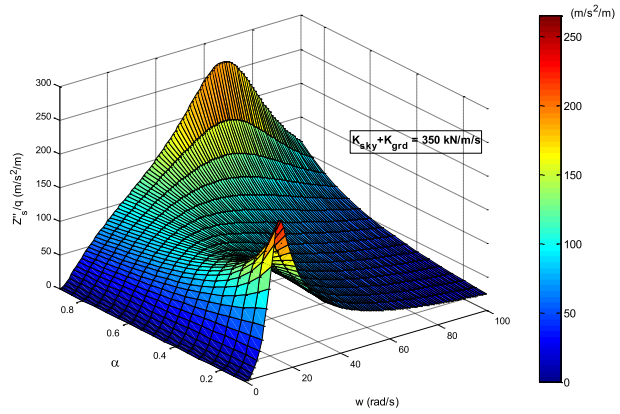

FIGURE 5. Frequency-response characteristics of sprung mass acceleration.

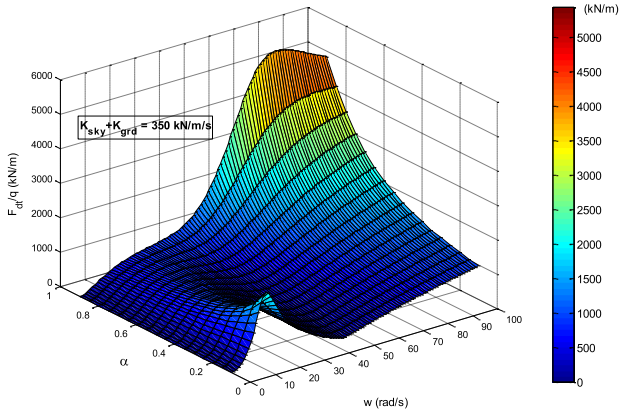

FIGURE 6. Frequency-response characteristics of dynamic tyre force.

comfort by adjusting the damping force based on the relative velocity of the mass. When facing challenging driving situations on rough terrains where the unsprung mass oscillates significantly, the control system automatically switches to the Groundhook mode, which concentrates on directly controlling the interaction between the wheels and the road surface to optimize road holding, vehicle stability, and performance. By integrating both modes, the proposed HASS employs the control force as suggested in equation (12).

The control quality of the HASS depends significantly on the values of the parameters K_{sky}, K_{grd} and α. In this section, the study focuses on examining the variation of K_{sky} within the range of 0 to 6000 Ns/m, K_{grd} within the range of 0 to 12000 Ns/m, with three values of α being 0.3, 0.6, and 0.9, respectively. The evaluation criterion used in this study is the root mean square (rms) of signals such as displacement and acceleration of the sprung mass, unsprung mass, and the dynamic tyre force [39], [40], [41].

Figure 7 illustrates the variation in the magnitude of the rms of the sprung mass acceleration when K_{sky} and K_{grd} change. In general, an increase in K_{grd} leads to a gradual decrease in the acceleration of the sprung mass. For

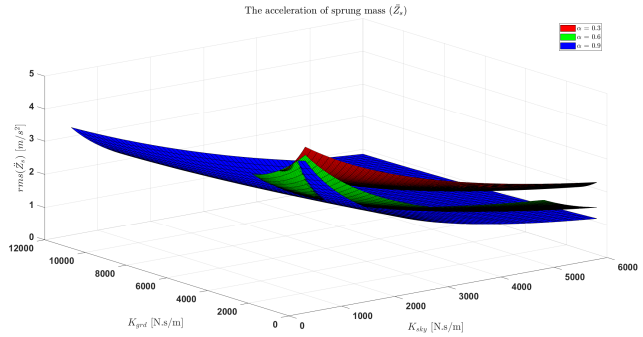

FIGURE 7. The survey results of the root mean square of the acceleration of the sprung mass.

$\alpha = 0.3$, the acceleration value decreases the most, followed by $\alpha = 0.6$ and finally $\alpha = 0.9$. When the value of α increases, the magnitude of this root mean square of the acceleration decreases. In summary, by simultaneously increasing both K_{sky} and K_{grd}, the amplitude of the acceleration of the sprung mass can be reduced.

Figure 8 illustrates the variation in the displacement of the sprung mass when the values of K_{sky} and K_{grd} change. The trend of the displacement of the sprung mass is similar to its acceleration. When both K_{sky} and K_{grd} increase, the displacement of the sprung mass decreases.

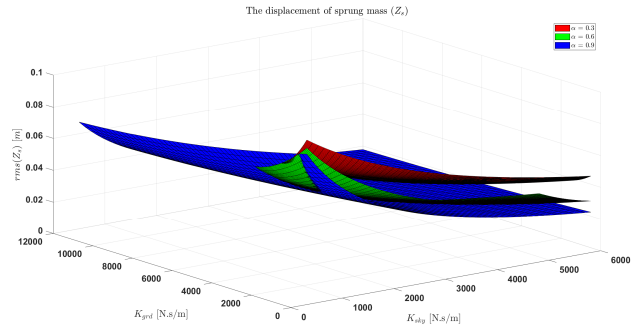

FIGURE 8. The survey results of the root mean square of the displacement of the sprung mass.

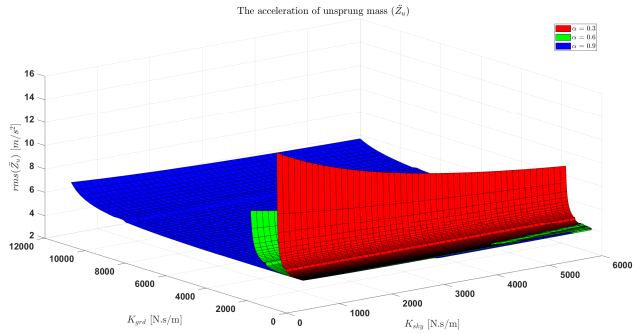

FIGURE 9. The survey results of the root mean square of the acceleration of the unsprung mass.

Figure 9 illustrates the variation of the acceleration of the unsprung mass as K_{sky} and K_{grd} change. When the value of

K_{grd} increases, this acceleration also increases. Specifically, in the case of $\alpha = 0.3$, the acceleration of unsprung mass has the highest on its rms value, followed by $\alpha = 0.6$, and finally $\alpha = 0.9$. When the value of K_{sky} increases, the rms acceleration of unsprung mass tends to decrease steadily. In summary, increasing K_{grd} will raise the acceleration of the unsprung mass.

Figure 10 illustrates the variation of the unsprung mass displacement as K_{sky} and K_{grd} change. When the value of K_{grd} increases, this displacement decreases. Specifically, in the case of $\alpha = 0.3$, the displacement decreases the most, followed by $\alpha = 0.6$, and finally $\alpha = 0.9$. Meanwhile, gradually increasing the value of K_{sky} in all three cases of α, the value of Z_u decreases, although not significantly. In conclusion, increasing the values of K_{sky} and K_{grd} will reduce the displacement of the unsprung mass.

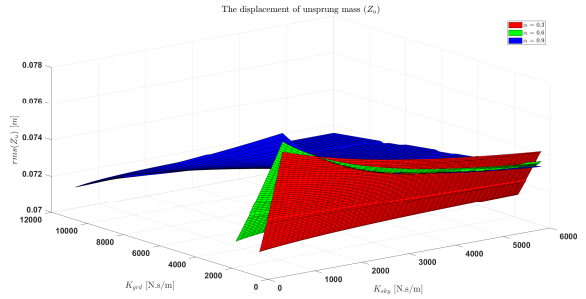

FIGURE 10. The survey results of the root mean square of the displacement of the unsprung mass.

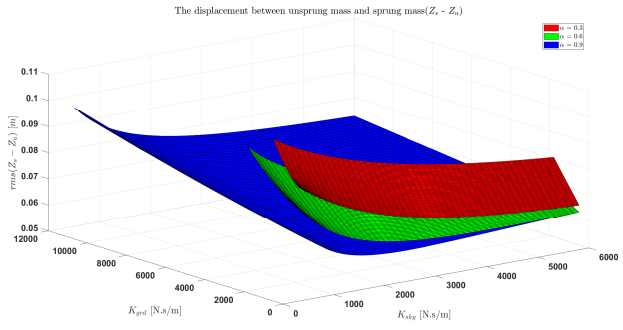

FIGURE 11. The survey results of the root mean square of the displacement of the suspension system.

Figure 11 shows the variation in vertical displacement between the unsprung mass and the sprung mass when the values of K_{sky} and K_{grd} change. When K_{grd} increases, the displacements of all cases increase uniformly. In particular, in the case of $\alpha = 0.3$, this displacement increases most significantly, followed by $\alpha = 0.6$, and finally $\alpha = 0.9$. Meanwhile, the increment of K_{sky} in the cases of $\alpha = 0.3, 0.6$ cause increases. Nevertheless, for $\alpha = 0.9$ specifically, $RMS\ (Z_s - Z_u)$ decreases as K_{sky} ranges 500 to $2408Ns/m$, and from $K_{sky} = 2408Ns/m$ onwards, $RMS\ (Z_s - Z_u)$ increases.

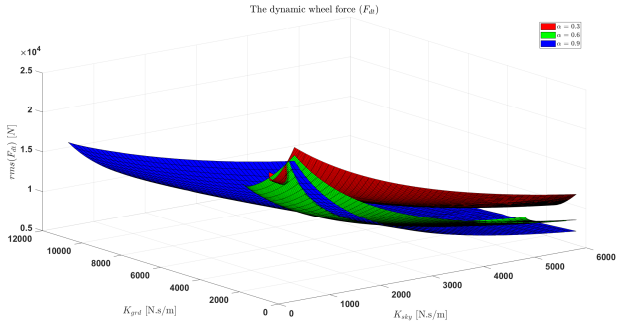

FIGURE 12. The survey results of the root mean square of the displacement of the dynamic tyre force.

Figure 12 illustrates the variation in the dynamic tyre force with changes in K_{sky} and K_{grd}. When K_{grd} increase with $\alpha = 0.9, 0.6$, this force decreases; with $\alpha = 0.3$, the force F_{dt} initially decreases and then rises again. As K_{sky} increases, F_{dt} decreases in all three cases of $\alpha = 0.9, 0.6, 0.3$.

TABLE 2. Summary of results of evaluation of the impact of K_{SKY}, K_{GRD} coefficients.

Symbol	$\ddot{Z}_s$	Z_s	$\ddot{Z}_u$	Z_u	$Z_s - Z_u$	F_{dt}
K_{sky} *increases*	↓	↓	↓	↓	↓	↓
K_{grd} *increases*	↓	↓	↑	↓	↑	↓

Table 2 is a summary of research results, a relative assessment when increasing the coefficients K_{sky}, K_{grd} to receive values of increasing magnitude. The upward arrows show that the root mean square value of the signals increases as the K_{sky}, K_{grd} coefficients increase. Conversely, the downward arrows show that the root mean square value of the signals decreases as the K_{sky}, K_{grd} coefficients increase.

The results of the investigation into the variations of K_{sky}, K_{grd} and α demonstrate a significant impact of these parameters on the ASS using the Hybrid control. Therefore, combining optimization methods with the Hybrid control model is necessary to enhance the effectiveness of the system to improve both road holding and ride comfort.

V. DEVELOP OPTIMAL HYBRID ACTIVE SUSPENSION SYSTEM BY GENETIC ALGORITHM

During the vehicle's movement on the road, the HASS will require adaptive control weighting parameter α to fit various operating conditions. Therefore, it can provide a flexible and effective solution, ensuring ride comfort and road safety criteria for the driver and passengers across different terrains and driving conditions. In the conventional control model of the ASS, through trial and error, the authors propose adjusting the weighting parameter $\alpha = 0.6$ to establish a reasonable relationship between ride comfort and road holding.

However, this is not yet an optimal solution to conserve energy supplied to the controller and balance the conflicting criteria of ride comfort and road holding. In this section, the authors propose a multi-objective optimization model using GA to optimize the coefficient K_{sky} and K_{grd} for the proposed HASS as described in Figure 13.

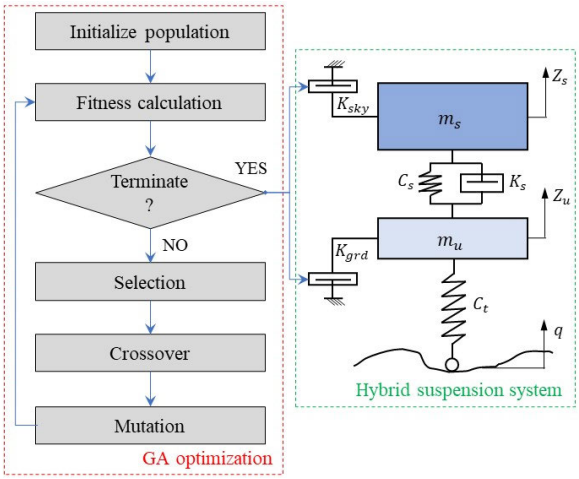

FIGURE 13. Structural diagram using GA to optimize HASS.

GA is an optimization method inspired by the natural evolutionary process. In the problem of finding coefficients K_{sky} and K_{grd} for the HASS, GA operates through a specific process. First, an initial population of individuals is established, with each individual representing a set of values for K_{sky} and K_{grd}. Then, each individual is evaluated by calculating the loss function or utility function based on these two coefficients within the range of $K_{sky} = \begin{bmatrix} 1000 & 10000 \end{bmatrix}$ and $K_{grd} = \begin{bmatrix} 100 & 15000 \end{bmatrix}$. Next, individuals are selected based on the rms value of the sprung mass acceleration $\ddot{Z}_s$ representing the ride comfort evaluation criterion and the acceleration value of the unsprung mass $\ddot{Z}_u$ representing the motion safety evaluation criterion to proceed to the next generation. The selected individuals then undergo crossover and mutation operations to generate new offspring to filter K_{sky} and K_{grd} values that satisfy the limit thresholds $\ddot{Z}_s < 2m/s^2$, $\ddot{Z}_u < 4m/s^2$ and $F_{dt} \to 0N$. This process is repeated over 50 generations until the stopping condition achieves the function f according to equation (13). This results in the final optimal solution for the problem of finding coefficients K_{sky} and K_{grd}.

$$\begin{aligned} f &= (1-\beta)J_{Comfort} + \beta J_{RoadHolding} \\ &= (1-\beta)\text{rms}(\ddot{Z}_s) + \beta\text{rms}(\ddot{Z}_u), \forall\beta \in \begin{bmatrix} 0 & 1 \end{bmatrix} \end{aligned} \quad (13)$$

In equation (13), β represents the optimal weighting parameter for the multi-objective GA optimization problem. Figure 14 illustrates the Pareto function f values obtained when varying β. Thus, for each different value of β the multi-objective GA will select the optimal pair of K_{sky} and K_{grd} for the model. To visually represent these criteria, the authors chose three sets of parameters $\beta = 0.1$, $\beta = 0.5$ and $\beta = 0.9$ corresponding to prioritizing ride comfort ($\beta = 0.1$), balancing both ride comfort and road holding ($\beta = 0.5$), and prioritizing road holding ($\beta = 0.9$).

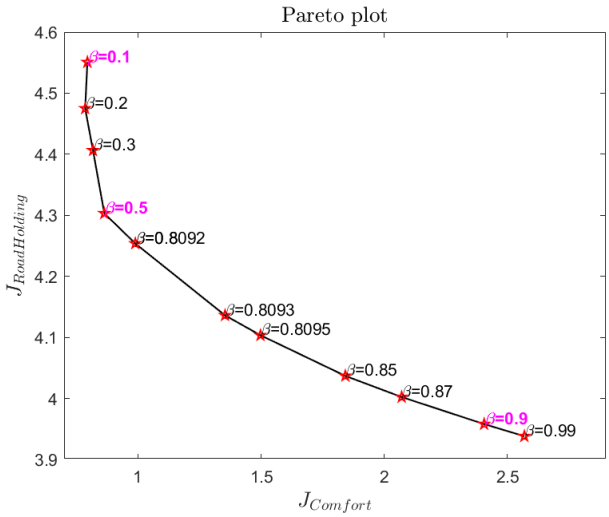

FIGURE 14. Pareto of function f values.

Table 3 compiles the optimized results obtained using the GA method for the coefficients K_{sky} and K_{grd}. In the subsequent section, the authors will simulate, evaluate, and compare the effectiveness of the HASS in its non-optimized state, its optimized state with specific values $\beta = 0.1$, $\beta = 0.5$, $\beta = 0.9$ and passive suspension system across both the frequency and time domains.

TABLE 3. Optimization results of coefficients K_{sky} and K_{grd} using GA.

	$\beta = 0.1$	$\beta = 0.5$	$\beta = 0.9$
K_{sky}	9501.4023	9678.6895	2275.4474
K_{grd}	1996.0165	1106.1185	1001.6251

VI. EVALUATION OF THE EFFECTIVENESS OF THE HYBRID ACTIVE SUSPENSION SYSTEM

A. ANALYSIS IN THE FREQUENCY DOMAIN

Figure 15 illustrates the variation in the magnitude of the rms value of acceleration and displacement of the sprung mass when the frequency changes from 0 Hz to 20 Hz. The authors chose for the excitation source a sinusoidal periodic waveform with an amplitude of 0.1 meters, while the frequency is varied. The solid black line represents the values of the uncontrolled model (Passive), and the solid red line represents the results of the controlled model without optimizing the parameters K_{sky} and K_{grd} (Active), and the solid green, dashed blue, and dotted light blue lines respectively represent the results of the model integrated with the GA algorithm selecting optimized coefficient and when ($\beta = 0.1$, $\beta = 0.5$, $\beta = 0.9$). It is observed that the results of the uncontrolled model consistently exhibit higher values compared to the

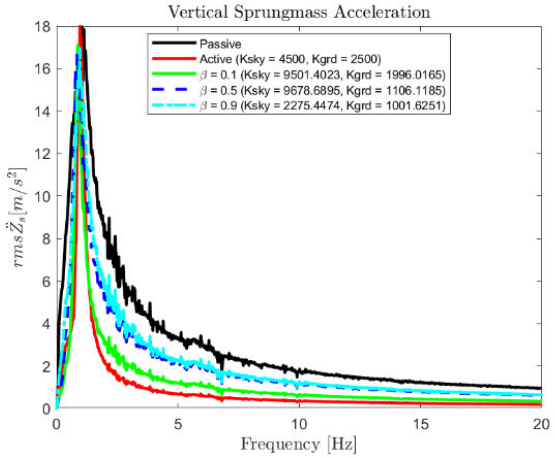

a)

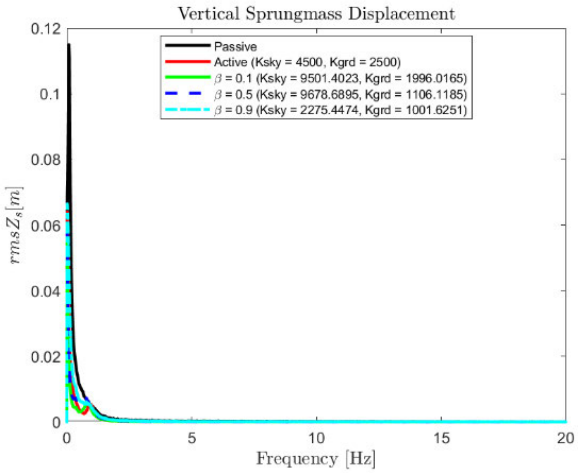

b)

FIGURE 15. Frequency response of the root means square of: a) Acceleration of the sprung mass; b) Displacement of the sprung mass.

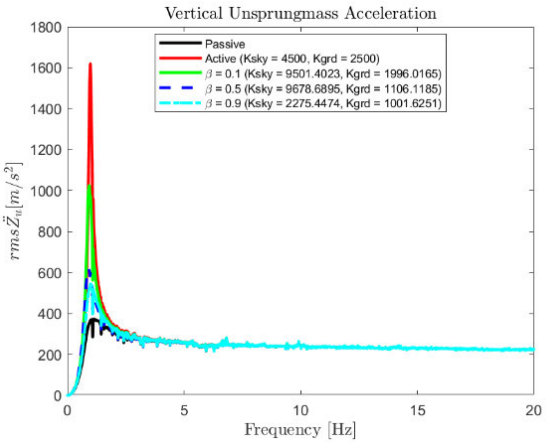

a)

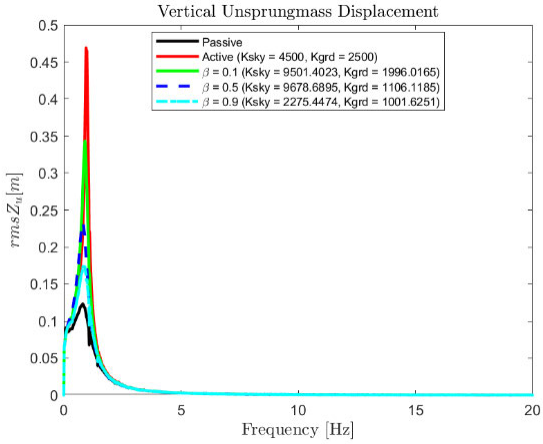

b)

FIGURE 16. Frequency response of the root means square of: a) Acceleration of the unsprung mass; b) Displacement of the unsprung mass.

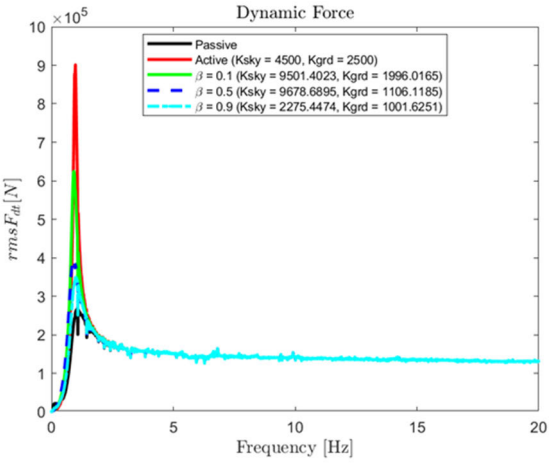

FIGURE 17. Frequency response of root means square of the dynamic tyre force.

controlled model, demonstrating that the proposed model has advantages in reducing the magnitude of the desired signal in the frequency domain.

In the frequency range of 1-2 Hz, the rms magnitude values of the sprung mass tend to resonate. However, by using the GA algorithm to select coefficients K_{sky} and K_{grd} that balance between ride comfort and road holding criteria for the vehicle, the system can still maintain necessary constraints. It is observed that as β increases gradually from 0.1 to 0.9, the rms value of the acceleration of the sprung mass increases. This indicates a decreasing priority towards ride comfort criteria. Similarly, the displacement signal of the sprung mass in this frequency range exhibit similar trends.

When evaluating the characteristics of the sprung mass in a higher frequency range from 5 Hz to 20 Hz, it is observed that the rms value of the acceleration lean towards decreasing. The largest decrease is seen in the non-optimized active control model, followed by the GA-optimized models with $\beta = 0.1$, $\beta = 0.5$, and $\beta = 0.9$. Meanwhile, the rms values of the displacement approach zero. Figure 16 presents the

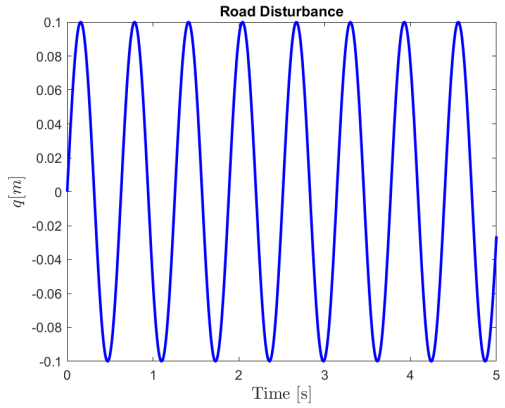

FIGURE 18. Road disturbance in simulation quarter vehicle model.

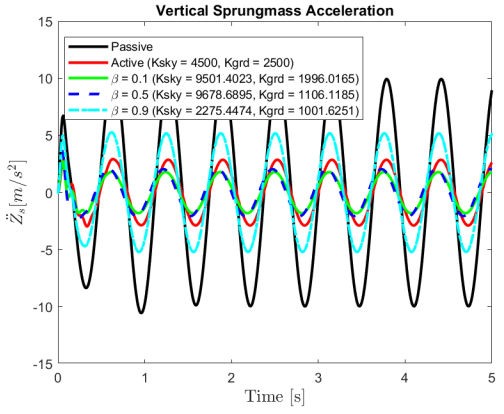

a)

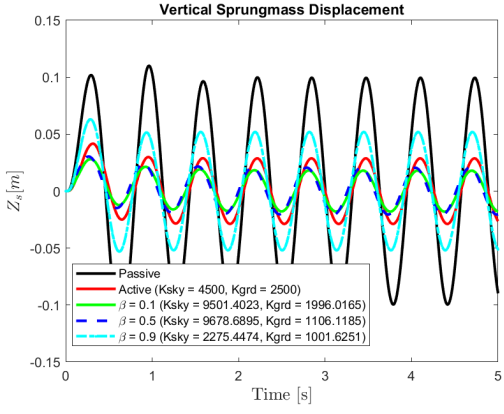

b)

FIGURE 19. Time response of: a) Sprung mass acceleration; b) Sprung mass displacement.

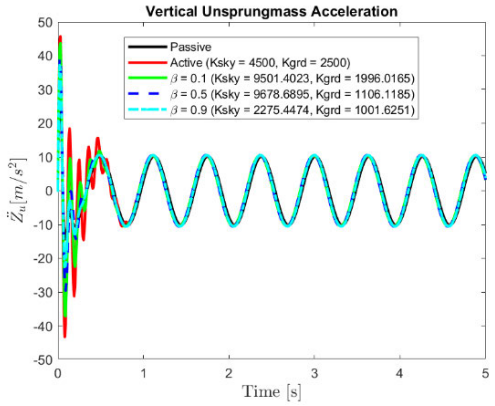

a)

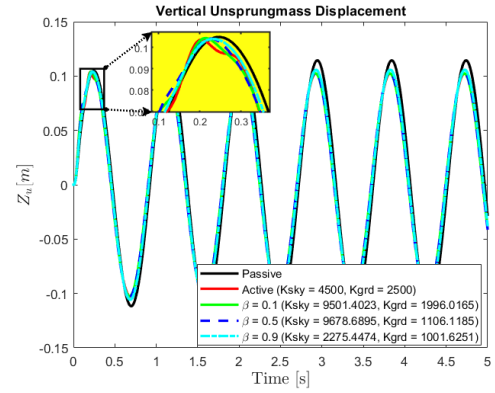

b)

FIGURE 20. Time response of: a) Unsprung mass acceleration; b) Unsprung mass displacement.

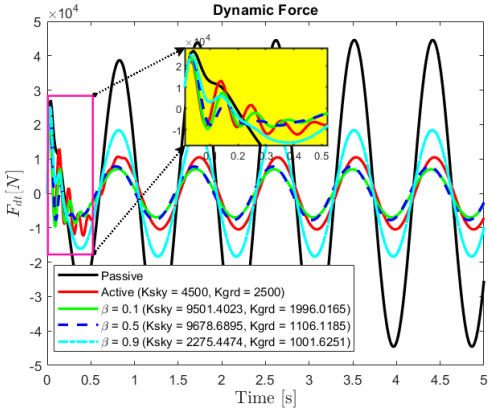

FIGURE 21. Comparison of the root means square for dynamic tyre force.

frequency response from 0 Hz to 20 Hz of the rms values for the acceleration of the unsprung mass (Figure 16a) and the displacement of the unsprung mass (Figure 16b). The results show that the low-frequency resonance region of the unsprung mass is about 1 rad/s to 2 rad/s. In this region, the root mean square value of displacement and acceleration increases sharply, which shows the strong oscillation of the wheel in this frequency region, and it makes the wheel at risk of being lifted off the road surface.

Figure 17 demonstrates the frequency response of the rms values of the dynamic tyre force from 0 Hz to 20 Hz. It is observed that at low frequencies ranging from 1 Hz to 2 Hz, the dynamic tyre force is influenced by road excitation, leading to a significant peak in the rms values. Specifically, the

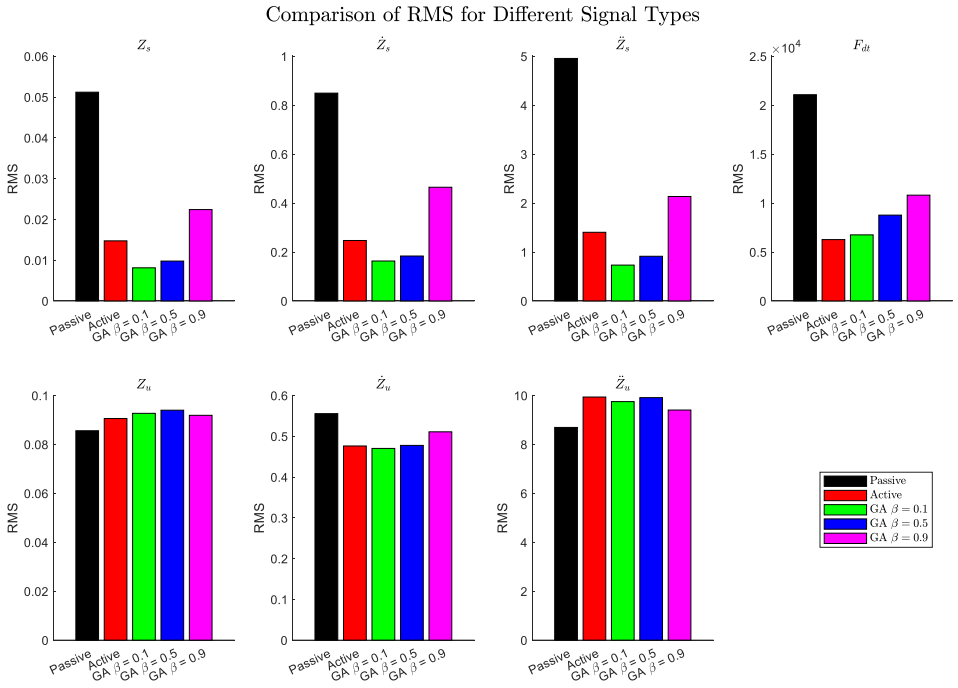

FIGURE 22. Comparison of the root means square value for each referred signal.

non-optimized control model exhibits the highest peak reaching approximately 90 kN, followed by the GA-optimized models with weights $\beta = 0.1$, $\beta = 0.5$ and $\beta = 0.9$; and finally the uncontrolled suspension system. In higher frequency ranges, the rms value of the dynamic tyre force across all models rapidly decreases and stabilizes around 1.85 kN at frequencies above 10 Hz.

B. ANALYSIS IN THE TIME DOMAIN

In this section, a quarter-vehicle model is analyzed under the influence of harmonic oscillations resembling a sine wave with an amplitude of 0.1 meters and a frequency of 7 rad/s, as shown in Figure 18. Figure 19 presents the time responses of the suspension system in terms of sprung mass acceleration (Figure 19a) and displacement of the sprung mass (Figure 19b).

It is observed that in the passive suspension system, the acceleration and displacement of the sprung mass exhibit very large amplitudes, reaching approximately 10 m/s^2 and 0.1 meters, respectively. In contrast, with a controlled suspension system, the amplitudes of these signals related to the sprung mass are significantly reduced by over 80%. Among the controlled models integrated with the GA algorithm, the controller with $\beta = 0.1$ achieves the smallest acceleration amplitude, followed by the controller with $\beta = 0.5$ and the lowest is the controller with $\beta = 0.9$. Despite the integration of the GA algorithm, the GA-controlled system with $\beta = 0.9$ demonstrates a clearer tendency to optimize for safety criteria while neglecting ride comfort criteria. Consequently, the amplitudes of the acceleration and displacement signals of the sprung mass for this GA-controlled system are larger compared to the conventional controlled system.

Figure 20 presents simulation results comparing the effectiveness of the proposed models in the time domain of the unsprung mass. The controlled suspension system models demonstrate significant effectiveness in reducing the amplitude of the unsprung mass accleration. Specifically, the model integrated with the GA algorithm by selecting $\beta = 0.5$ achieves amplitude of unsprung mass displacement equivalent to that of the conventional controlled model.

The acceleration and displacement signals of the unsprung mass exhibit trends opposite to those of the velocity signal of the sprung mass. By comparing the rms value of these signals with the uncontrolled model, there is a slight increase in the magnitude of the one's values. However, the extent of the increase and the magnitude of the rms values of the unsprung mass remain within acceptable limits to ensure safety criteria without compromising the durability requirements of this component.

In various operating conditions, the dynamic tyre force is considered a critical factor and plays a key role in assessing the road holding of vehicles. Figure 21 compares the dynamic tyre force of the proposed models with the passive suspension system model. It is observed that all proposed models effectively reduce the dynamic force, with the conventionally controlled model achieving the greatest reduction of up to 76%, followed by the model with additional GA-integrated control using $\beta = 0.1$, $\beta = 0.5$ and $\beta = 0.9$.

The synthesized results of the rms values of the time response signals in the proposed model are detailed in

Figure 22. It can be observed that the reduction in rms values of the signals ($\ddot{Z}_s$, $\dot{Z}_s$, Z_s) related to ride comfort ranges from 60% to 80% depending on the different values of the coefficients K_{sky} and K_{grd}. When considering passenger comfort, the vehicle utilizing the Hybrid control model with optimized coefficients demonstrates the highest effectiveness. Regarding road safety criteria related to the dynamic tyre force, the Hybrid control suspension system significantly outperforms the passive suspension system. As for criteria related to the road holding, the differences in rms values ($\ddot{Z}_u$, $\dot{Z}_u$, Z_u, F_{dt}) range from 10% to 15%.

The simulation and evaluation results in both the time and frequency domains clearly demonstrate the effectiveness of the actively controlled suspension system using the Hybrid ASS model. The optimization results obtained through the GA method allow the determination of essential coefficients of the HASS, thereby conducting the system effectively towards enhancing ride comfort and road holding objectives. Based on this, methods can be proposed to adaptively adjust the control model coefficients to different vehicle operating conditions.

VII. CONCLUSION

This article presents an in-depth study on designing a controller for the active suspension system using a HASS model by combining the Skyhook and Groundhook models. Firstly, the ASS model with an electro-hydraulic actuator is detailed. Subsequently, the HASS model is described and fully established using various transfer functions. The parameters of the HASS are optimized through a GA method to enable the system's vertical stability to adapt to different conditions. Evaluation results demonstrate that there is a reduction in root mean square values of ride comfort-related signals by 60% to 80% and road safety-related signals by 10% to 15% depending on different coefficients K_{sky} and K_{grd}. Afterthat, the study two high level parameters α, β in the HASS model and optimizing them with GA approach allowed for the identification of control parameters optimally geared towards enhancing neither road holding nor ride comfort. This represents a completely novel approach compared to previous studies on ASS in vehicles.

The next research direction to complete this system could be to use a controller that can convert α and β coefficients according to different vehicle motion conditions. Besides, considering the use of multi-objective genetic algorithms and other methods for the HASS system is also a potential research direction.

ACKNOWLEDGMENT

The authors would like to extend their sincere gratitude to the National Research, Development, and Innovation Office; the Embassy of Hungary in Vietnam; the colleagues with the Department of Automotive Mechanical Engineering, Faculty of Mechanical Engineering, University of Transport and Communications; the Faculty of Mechanical-Automotive and Civil Engineering, Electric Power University; and the Systems and Control Laboratory, Institute for Computer Science and Control (SZTAKI), Hungarian Research Network, Budapest, Hungary, for their support and assistance in enabling them to complete this research.

REFERENCES

[1] S. M. Savaresi, C. P.-V. C. Spelta, and O. S. L. Dugard, *Semi-Active Suspension Control Design for Vehicles*. Butterworth-Heinemann, 2010.
[2] S. Fergani, "Robust multivariable control for vehicle dynamics," Ph.D. dissertation, Grenoble Alpes Univ., GIPSA-Lab, Grenoble, France, 2014. [Online]. Available: https://theses.hal.science/tel-01303752
[3] O. Sename, "Review on LPV approaches for suspension systems," *Electronics*, vol. 10, no. 17, p. 2120, Aug. 2021.
[4] V. Van Tan, "Two-layer parallel fuzzy logic controller design for semiactive suspension system with a full car model," *Shock Vibrat.*, vol. 2023, pp. 1–19, May 2023, doi: 10.1155/2023/7020462.
[5] M. Yu, S. A. Evangelou, and D. Dini, "Advances in active suspension systems for road vehicles," *Engineering*, vol. 33, pp. 160–177, Feb. 2024, doi: 10.1016/j.eng.2023.06.014.
[6] J. Y. Wong, *Theory of Ground Vehicles*, 5th ed. Hoboken, NJ, USA: Wiley, 2022.
[7] M. Menezes Morato, T.-P. Pham, O. Sename, and L. Dugard, "Development of a simple ER damper model for fault-tolerant control design," *J. Brazilian Soc. Mech. Sci. Eng.*, vol. 42, no. 10, pp. 1–12, Oct. 2020, doi: 10.1007/s40430-020-02585-y.
[8] T.-P. Pham, O. Sename, L. Dugard, and V. T. Vu, "LPV force observer design and experimental validation from a dynamical semi-active ER damper model," *IFAC-PapersOnLine*, vol. 52, no. 17, pp. 60–65, 2019, doi: 10.1016/j.ifacol.2019.11.027.
[9] M. Q. Nguyen, "LPV approaches for modelling and control of vehicle dynamics: Application to a small car pilot plant with ER dampers," Ph.D. dissertation, GIPSA-lab, Grenoble Alpes Univ., Grenoble, France, 2017. [Online]. Available: https://hal-bioemco.ccsd.cnrs.fr/GIPSA-SLR/tel-01470984v2
[10] C. Poussot-Vassal, O. Sename, L. Dugard, R. Ramirez-Mendoza, and L. Flores, "Optimal skyhook control for semi-active suspensions," *IFAC Proc. Volumes*, vol. 39, no. 16, pp. 608–613, 2006, doi: 10.3182/20060912-3-de-2911.00106.
[11] R.-K. Kim and K.-S. Hong, "Skyhook control using a full-vehicle model and four relative displacement sensors," in *Proc. Int. Conf. Control, Autom. Syst.*, 2007, pp. 268–272, doi: 10.1109/iccas.2007.4406920.
[12] T. Yuvapriya and P. Lakshmi, "Active suspension control of full car model using bat optimized PID controller," in *Artificial Intelligence Applications in Battery Management Systems and Routing Problems in Electric Vehicles*. Hershey, PA, USA: IGI Global, 2023, pp. 150–190, doi: 10.4018/978-1-6684-6631-5.ch008.
[13] Z. Boulaaras, A. Aouiche, and K. Chafaa, "PID controller optimized by using genetic algorithm for active suspension system of a quarter car," in *Proc. 19th Int. Multi-Conference Syst., Signals Devices (SSD)*, May 2022, pp. 779–784, doi: 10.1109/SSD54932.2022.9955858.
[14] W. Yu, K. Zhu, and Y. Yu, "Variable universe fuzzy PID control for active suspension system with combination of chaotic particle swarm optimization and road recognition," *IEEE Access*, vol. 12, pp. 29113–29125, 2024, doi: 10.1109/ACCESS.2024.3368762.
[15] D. T. Tu, V. Van Tan, O. Sename, and K. D. Thinh, "Designing a LQR controller for active suspension system of quarter heavy vehicle model with an electronic servo-valve hydraulic actuator," in *Proc. Int. Conf. Sustainable Energy Technol.* Springer, 2023, pp. 236–242.
[16] D.-V. Ahn, K. Kim, J. Oh, J. Seo, J. W. Lee, and Y.-J. Park, "Optimal control of semi-active suspension for agricultural tractors using linear quadratic Gaussian control," *Sensors*, vol. 23, no. 14, p. 6474, Jul. 2023, doi: 10.3390/s23146474.
[17] J. Wang, M. Zhou, J. Tong, J. Liu, and S. Chen, "Augmented Kalman estimator and equivalent replacement based Taylor series-LQG control for a magnetorheological semi-active suspension," *Actuators*, vol. 13, no. 4, p. 138, Apr. 2024, doi: 10.3390/act13040138.
[18] M. Park, Y. Jeong, and S. Yim, "Design of a modal controller with simple models for an active suspension system," *IEEE Access*, vol. 10, pp. 65585–65597, 2022, doi: 10.1109/ACCESS.2022.3184005.

[19] S. Manna, G. Mani, S. Ghildiyal, A. A. Stonier, G. Peter, V. Ganji, and S. Murugesan, "Ant colony optimization tuned closed-loop optimal control intended for vehicle active suspension system," *IEEE Access*, vol. 10, pp. 53735–53745, 2022, doi: 10.1109/ACCESS.2022.3164522.

[20] L. Ovalle, H. Ríos, and H. Ahmed, "Robust control for an active suspension system via continuous sliding-mode controllers," *Eng. Sci. Technol., Int. J.*, vol. 28, Apr. 2022, Art. no. 101026, doi: 10.1016/j.jestch.2021.06.006.

[21] Y. Yin, B. Luo, H. Ren, Q. Fang, and C. Zhang, "Robust control design for active suspension system with uncertain dynamics and actuator time delay," *J. Mech. Sci. Technol.*, vol. 36, no. 12, pp. 6319–6327, Dec. 2022, doi: 10.1007/s12206-022-1143-1.

[22] K. K. Afshar, R. Korzeniowski, and J. Konieczny, "Constrained dynamic output-feedback robust H_∞ control of active inerter-based half-car suspension system with parameter uncertainties," *IEEE Access*, vol. 11, pp. 46051–46072, 2023, doi: 10.1109/ACCESS.2023.3272328.

[23] G. Kim, S. Y. Lee, J.-S. Oh, and S. Lee, "Deep learning-based estimation of the unknown road profile and state variables for the vehicle suspension system," *IEEE Access*, vol. 9, pp. 13878–13890, 2021, doi: 10.1109/ACCESS.2021.3051619.

[24] E. Sabanovič, P. Kojis, S. Sukevičius, B. Shyrokau, V. Ivanov, M. Dhaens, and V. Skrickij, "Feasibility of a neural network-based virtual sensor for vehicle unsprung mass relative velocity estimation," *Sensors*, vol. 21, no. 21, p. 7139, Oct. 2021, doi: 10.3390/s21217139.

[25] E. Sabanovič, P. Kojis, V. Ivanov, M. Dhaens, and V. Skrickij, "Development and evaluation of artificial neural networks for real-world data-driven virtual sensors in vehicle suspension," *IEEE Access*, vol. 12, pp. 13183–13195, 2024, doi: 10.1109/ACCESS.2024.3356715.

[26] V. S. Payghan, P. D. Shendge, R. M. Yerge, and S. B. Phadke, "Skyhook control for active suspension system with a novel variable damper," in *Proc. 2nd IEEE Int. Conf. Recent Trends Electron., Inf. Commun. Technol. (RTEICT)*, May 2017, pp. 725–729, doi: 10.1109/RTEICT.2017.8256692.

[27] F. Kou, Q. Jing, C. Chen, and J. Wu, "Endocrine composite skyhook-groundhook control of electromagnetic linear hybrid active suspension," *Shock Vibrat.*, vol. 2020, pp. 1–17, Feb. 2020, doi: 10.1155/2020/3402168.

[28] Q. Meng, C. Chen, P. Wang, Z. Sun, and B. Li, "Study on vehicle active suspension system control method based on homogeneous domination approach," *Asian J. Control*, vol. 23, no. 1, pp. 561–571, Jan. 2021, doi: 10.1002/asjc.2242.

[29] V. T. Vu and P. Gaspar, "Performance and robustness assessment of H_∞ active anti-roll bar control system by using a software environment," *IFAC-PapersOnLine*, vol. 52, no. 5, pp. 255–260, 2019, doi: 10.1016/j.ifacol.2019.09.041.

[30] V.-T. Vu, O. Sename, L. Dugard, and P. Gaspar, "H_∞ active anti-roll bar control to prevent rollover of heavy vehicles: A robustness analysis," *IFAC-PapersOnLine*, vol. 49, no. 9, pp. 99–104, 2016, doi: 10.1016/j.ifacol.2016.07.503.

[31] C.-S. Ting, T.-H.-S. Li, and F.-C. Kung, "Design of fuzzy controller for active suspension system," *Mechatronics*, vol. 5, no. 4, pp. 365–383, Jun. 1995, doi: 10.1016/0957-4158(95)00014-v.

[32] W. Zhao and L. Gu, "Hybrid particle swarm optimization genetic LQR controller for active suspension," *Appl. Sci.*, vol. 13, no. 14, p. 8204, Jul. 2023, doi: 10.3390/app13148204.

[33] A. Zaremba, R. Hampo, and D. Hrovat, "Optimal active suspension design using constrained optimization," *J. Sound Vibrat.*, vol. 207, no. 3, pp. 351–364, Oct. 1997, doi: 10.1006/jsvi.1997.1117.

[34] H. Metered, W. Abbas, and A. S. Emam, "Optimized proportional integral derivative controller of vehicle active suspension system using genetic algorithm," *SAE Technical Papers*, vol. 2018, pp. 1–8, Apr. 2018, doi: 10.4271/2018-01-1399.

[35] L. R. C. Drehmer, W. J. Paucar Casas, and H. M. Gomes, "Parameters optimisation of a vehicle suspension system using a particle swarm optimisation algorithm," *Vehicle Syst. Dyn.*, vol. 53, no. 4, pp. 449–474, Apr. 2015, doi: 10.1080/00423114.2014.1002503.

[36] M. Nagarkar, Y. Bhalerao, G. V. Patil, and R. Z. Patil, "Multi-objective optimization of nonlinear quarter car suspension system—PID and LQR control," *Proc. Manuf.*, vol. 20, pp. 420–427, Jan. 2018, doi: 10.1016/j.promfg.2018.02.061.

[37] V. Van Tan, O. Sename, L. Dugard, and P. Gaspar, "Optimal selection of weighting functions by genetic algorithms to design H_∞ anti-roll bar controllers for heavy vehicles," in *Proc. Mini Conf. Vehicle Syst. Dyn., Identificat. Anomalies*, Nov. 2016, pp. 23–37.

[38] T. Van Nhu, "Computer application to solve vehicle vibration problems," Univ. Transp. Commun., Hanoi, Vietnam, Tech. Rep., 2003.

[39] V. V. Tan, T. M. Hung, and O. Sename, "An investigation into the ride comfort of buses using an air suspension system," *Int. J. Heavy Vehicle Syst.*, vol. 28, no. 2, pp. 184–205, 2021, doi: 10.1504/ijhvs.2021.115595.

[40] V. V. Tan, O. Sename, and P. Gáspár, "Improving roll stability of tractor semi-trailer vehicles by using H_∞ active anti-roll bar control system," *Proc. Inst. Mech. Eng., D, J. Automobile Eng.*, vol. 235, no. 14, pp. 3509–3520, Dec. 2021, doi: 10.1177/09544070211013949.

[41] V. Van Tan, O. Sename, P. Gaspar, and T. Tu Do, *Act. Anti-Roll Bar Control Design for Heavy Vehicles*. Berlin, Germany: Springer, 2014, doi: 10.1007/978-981-97-1359-2.

VU VAN TAN was born in Nam Định, Vietnam, in 1985. He received the B.E. and master's degrees in mechanical engineering, in 2008 and 2012, respectively, and the Ph.D. degree from the Gipsa-Laboratory, Grenoble Alpes University, in 2017.

Since 2008, he has been a Lecturer with the Department of Automotive Mechanical Engineering, Faculty of Mechanical Engineering, University of Transport and Communications (UTC), Hanoi, Vietnam. Since 2021, he has been an Associate Professor with the Department of Automotive Mechanical Engineering. He has published more than 40 journal articles, one monograph book, three domestic books, one book chapter, and ten conference proceedings papers: vehicle dynamics and control; vehicle stability/safety; and electric/autonomous vehicles. He was the Key Manager of a numerical project on vehicle engineering at university key level, in 2010, 2012, 2019, 2020, and 2022. Particularly, from 2018 to 2019, he was a main researcher with Vietnamese side on international research project supported by French Embassy in Vietnam. Currently, he is the (co-)supervisor of four Ph.D. and five master students. He was the organizer of the workshops: The LPV Methods for Automotive Applications, in April 2017; the Linear Parameter Varying approach for Fault Tolerant Control design (LPV4FTC), in October 2017; the Gipsa-Laboratory, Grenoble, France. He was the Co-Chair of the International Scientific Conference on Sustainable Energy Technologies (ICSET2023), Industrial University of Ho Chi Minh City, Vietnam, in 2023.

DO TRONG TU was born in Nam Định, Vietnam, in 1998. He received the B.E. degree from UTC, in August 2020, and the Master of Science degree in mechanical engineering from Myongji University, South Korea, in 2023.

In 2020, he got an International Internship Program with the Gipsa-Laboratory, Grenoble INP, France, supervised by Prof. Olivier Sename, Prof. Luc Dugard, and Prof. Vu Van Tan. He participated in Transportation Traffic Construction and Mechanical Joint Stock Company, simultaneously with the Automotive Research and Training Support Center, Hanoi, Vietnam, as a Research Engineer, in 2020. Since 2021, he has been a Master/Researcher with the Advanced Automotive Laboratory with energy management systems for fuel cell electric vehicles. Currently, he is a Lecturer with Electric Power University, Hanoi. His research interests include vehicle dynamics and control and energy management systems for XEVs, including BEVs, HEVs, and FCEVs.

NGUYEN VAN VINH was born in Hanoi, Vietnam, in 2000. He received the B.E. degree from UTC, in April 2024, supervised by Assoc. Prof. Vu Van Tan.

His research interests include vehicle dynamics and control, optimization algorithms, deep learning, and autonomous vehicles.

PHAM TAT THANG was born in Hà Nam, Vietnam, in 1977. He received the B.E. and master's degrees in mechanical engineering, in 2000 and 2006, respectively, and the Ph.D. degree from the TEMPO-Laboratory, Valenciennes et du Hainaut-Cambresis University, under the supervision of Prof. Mirentxu Dubar and Prof. André Dubois, in 2015, with a thesis title "Endommagement en surface des alliages d'aluminium en mise en forme à froid."

Since 2001, he has been a Lecturer with the Department of Automotive Mechanical Engineering, Faculty of Mechanical Engineering, University of Transport and Communications, Hanoi, Vietnam. He has published more than ten journal papers, one book chapter, and (co-)supervised ten master students in automotive mechanical engineering. Currently, he is (co-)supervisor of one master and one Ph.D. students. His research interests include vehicle dynamics and control, vehicle stability/safety, and autonomous vehicles.

ANDRAS MIHALY was born in Budapest, Hungary, in 1981. He received the master's degree in transportation engineering and the Ph.D. degree in transportation sciences from Budapest University of Technology and Economics, in 2008 and 2022, respectively. He has been a Research Fellow with the Systems and Control Laboratory, Institute for Computer Science and Control (SZTAKI), Hungarian Research Network, since 2015. He has published more than 30 journal articles, one book chapter, and 39 papers in conference proceedings with more than 247 citations. His main fields of research interests include integrated vehicle control, in-wheel vehicle control, driver modeling, adaptive speed control, active and semi-active suspension control, vehicle platoon control, and reinforcement learning control for autonomous vehicles.

PETER GASPAR received the M.Sc. and Ph.D. degrees from BME, in 1985 and 1997, respectively, and the D.Sc. degree in control from Hungarian Academy of Sciences (MTA), in 2007.

He is currently the Head of the Systems and Control Laboratory, Institute for Computer Science and Control (SZTAKI), Hungarian Research Network. He is also a Full Professor with the Department of Control for Transportation and Vehicle Systems, Budapest University of Technology and Economics (BME). He is the Head of the BME Kalman Kandó Doctoral School. He is the Head of the National Laboratory for Autonomous Systems. He is the co-author of five monographs on systems and control theory and vehicle control and the co-author of seven university textbooks. He has 177 journal articles, seven book chapters, and 306 papers in conference proceedings with more than 2700 citations. His research and industrial works have involved mechanical systems, vehicle structures, and vehicle dynamics and control. He has played a leading role in several research and development projects, some of which are listed below: partially automated vehicle platforms with safety and economy features; design of fleet management systems for commercial vehicles; driver assistance distributed systems for commercial vehicle platforms; the development of intelligent adaptive speed control considering road and traffic conditions; variable geometry suspension mechanisms and control design; and research into artificial intelligence in the field of future mobility. He has also participated in several industrial projects, some of which are listed below: the development of a diagnostic system for reactors and primary loops; control design and implementation of an industrial pressurizer in a nuclear power plant; and the development of a safety, driver assistance, reliability, energy efficiency, and environmental awareness project. His research interests include linear and nonlinear systems, robust control, identification for control, machine learning, and reinforcement learning methods. From 2019 to 2023, he was a member of the Steering Committee of Eötvös Loránd Research Network. Since 2022, he has been a member of Hungarian Academy of Sciences. He is a member of the IFAC Automotive Control and Transportation Systems Technical Committees. He is a member of the University and Habilitation Committee of BME. He is the Chair of the IFAC Hungary National Member Organization.